Precision Agric (2013) 14:478–494
DOI 10.1007/s11119-013-9311-z

Automatic corn plant location and spacing measurement using laser line-scan technique

Yeyin Shi · Ning Wang · Randal K. Taylor · William R. Raun · James A. Hardin

Published online: 9 April 2013

Abstract Identifying corn plant location and/or spacing is important for predicting yield potential and making decisions for in-season nitrogen application rate. In this study, an automatic corn stalk identification system based on a laser line-scan technique was developed to measure stalk locations during corn mid-growth stages. A laser line-scan technique is advantageous in this application because the line-scan data sets taken from various points of view of a plant stalk results in less interference and higher probability of plant recognition. Data were collected for two 10-meter-long corn rows at the growth stages of V8 and V10 using a mobile test platform in 2011. Each potential stalk cluster was identified in a scan and registered with the same stalks in previous scans. The final location of a stalk was the average of the measured locations in all scans. The current system setup with data processing algorithms achieved 24.0 and 10.0 % of mean total errors in plant counting at the V8 and V10 growth stages, respectively. The root-mean-squared error (RMSE) between system measured plant locations and manually measured ones were 2.3 and 2.6 cm at the V8 and V10 growth stages, respectively. The interplant spacing measured by the developed system had a good correlation with the manual measurement with an R^2 of 0.962 and 0.951 for the V8 and V10 growth stages, respectively. This system can be ultimately integrated in a variable-rate-spraying system to improve real-time, high spatial resolution variable-rate nitrogen applications.

Keywords Corn population · In-field variability · Data clustering · Variable-rate technology

Y. Shi · N. Wang (✉) · R. K. Taylor · J. A. Hardin
Department of Biosystems and Agricultural Engineering, Oklahoma State University, 111 Agricultural Hall, Stillwater, OK 74078, USA
e-mail: ning.wang@okstate.edu

W. R. Raun
Department of Plant and Soil Sciences, Oklahoma State University, 044 Agricultural Hall, Stillwater, OK 74078, USA

Introduction

Nitrogen use efficiency (NUE) in cereal production worldwide is as low as 33 % (Raun and Johnson 1999). Much of the nitrogen (N) fertilizer applied to crops is lost to surface runoff and leaching. This results in environmental damage such as the contamination of groundwater supplies or eutrophication of surface waters.

Research on the approaches to reduce N losses has shown that the NUE decreases with increasing N application level (Gauer et al. 1992) and nitrate leaching can be significant when N is applied at rates in excess of that needed for maximum yield (Raun and Johnson 1995). These findings have motivated research and adoption of variable-rate N applications where N is applied during the growing season rather than being applied at a fixed rate prior to planting (Sowers et al. 1994).

It is critical to determine an optimal spatial scale for variable rate N application for in-field variability management. For corn production, Martin et al. (2005) evaluated by-plant corn yield variability based on the data collected in the USA, Argentina and Mexico from 2002 to 2004. The by-plant corn yield was calculated in the unit of kg/ha by assuming the grain yield of a plant was the average grain yield in an area of one hectare. The area occupied by that plant was calculated as half the distance to and from its two nearest neighbors multiplied by the row spacing. They reported an averaged standard deviation of plant to plant grain yield at 2 765 kg/ha. They also found that variability was not significant if the yield was averaged along the row over a scale greater than 0.5 m. These results indicated that high-resolution plant management protocols might have a significant impact in corn production.

Parameters commonly considered when investigating variability management are soil nutrient level, soil moisture, plant N content, plant population or spacing, plant height, canopy coverage or volume and canopy density. In corn production, variability of plant N content, plant population or spacing and plant height are often examined. Krall et al. (1977) found that every 2.5 cm increase in the standard deviation of plant spacing would decrease the yield by 210 kg/ha. Lauer and Rankin (2004) found that when the standard deviation in corn plant spacing was greater than 12.0 cm, relative grain yield reduced at 1.06 % with every centimeter increase of the standard deviation in plant spacing. A corn by-plant yield prediction model proposed by Martin et al. (2012) included plant height, plant spacing and normalized difference vegetative index (NDVI) and achieved an R^2 of 0.48. The previous model without using plant height and spacing had an R^2 of 0.22.

The research on plant population or interplant spacing measurement can be categorized as two types: airborne and ground-based (Dworak et al. 2011). Most of the airborne remote sensing approaches use hyperspectral or multispectral analysis to obtain large-scale data (Huang et al. 2010; Thorp et al. 2008). Ground-based sensing methods have been used for obtaining detailed crop and soil information. These can be done concurrently with other in-field operations such as planting, spraying or harvesting. Ground-based approaches for plant population or spacing measurements can be categorized as intrusive (mechanical methods) or non-intrusive methods.

Mechanical methods to measure corn plant population usually use the resistant force of stalks on a spring loaded arm or a gravity pendulum to count the number of stalks (Birrell and Sudduth 1995; Heege et al. 2004). Some of these methods have already been commercialized on combine harvesters. Non-intrusive methods are more suitable for sensing corn population at early and mid-growth stages. Some of these methods are based on capacitive sensing: Nichols (2000) invented a moisture detecting sensor installed on a combine head to count harvested stalks; Li et al. (2009) developed a capacitance biomass proximity sensor to count corn stalks during harvesting.

Other non-intrusive methods in ground-based crop sensing are mainly based on optical sensing technique including 2D color/gray-scale imaging and range sensing. Color imaging has been explored in several studies for corn plant counting and spacing measurement in the past few decades. Shrestha and Steward (2003, 2005) developed and tested a machine vision based corn plant population sensing system. Algorithms were developed for color image sequencing, segmentation and plant recognition in order to count corn plants and to estimate plant location and spacing. The root-mean-square errors (RMSEs) in population estimates were in the range of 5–6 % compared with manual counts. Tang and Tian (2008a, b) developed a real-time crop row image reconstruction and plant identification system for automatically measuring the spacing of emerged corn plants. They achieved an overall RMSE of 1.7 cm and an R^2 of 0.96. All of these studies targeted at early growth stage corn plants prior to canopy closure.

Range sensing techniques are another category of optical-based sensing methods that have been applied to crop parameter measurements. A photoelectric emitter and receiver pair is a 1D range sensor. Hummel et al. (2002) developed and tested photoelectric sensors installed on a combine corn head for plant diameter, spacing and population measurements. They used an air-jet system to physically remove corn leaves and other debris from the sensors' field of view. The average normalized population and spacing estimates were reported at 0.94 and 1.08, respectively. Luck et al. (2008) used an infra-red range sensor for in-field plant population measurements and achieved an error in population estimates between 0.7 and 4.4 %. They indicated that the main error source was the interference from leaves. A laser line scanner is a 2D range sensor. Wangler et al. (1994) patented a laser scanning sensor which could be attached on a sprayer to selectively spray according to the presence of the tree foliage. A laser scanning technique was also used for tree foliage density and wheat stand density estimation by calculating variation in laser penetration depth (Wei and Salyani 2004, 2004; Saeys et al. 2009).

Up to recent, little research has been conducted so far on corn plant location measurement in the mid-growth stages using 2D range sensing techniques. The objective of this study was to develop a system using the laser line-scan technique for automatic corn plant location measurements to facilitate in-season variable rate N applications. The specific objectives were to:

- Develop a data acquisition system based on laser line-scan techniques to obtain corn plant location and spacing information;
- Develop data processing algorithms to estimate corn plant location and spacing; and
- Evaluate the system performance at the V8 and V10 growth stages.

Materials and methods

System setup and principles

The data acquisition platform was a four-wheel cart which moved easily between rows (Fig. 1a). The key component of this system was a laser line scanner (LMS291, SICK AG, Waldkirch, Germany) which measured distances between the sensor and target objects based on the time-of-flight principle. It was configured to operate in continuous line scan mode with a field of view of 100° and a resolution of 0.25°. The laser scanner was mounted on the cart's front arm and aimed about 5-cm above the roots of the corn stalks with a downward angle of 20°. The scan plane formed a 70° angle with the plane of the plant row (Fig. 1c). This setup was selected to allow the sensing of stalks near the ground while maintaining sufficient clearance between the sensor and ground.

Multiple neighboring stalks within a row were sensed in a scan as illustrated in Fig. 1b. The number of stalks in a scan depended on the distance between the sensor and plant row, as well as how far apart neighboring plants were. A control program developed in

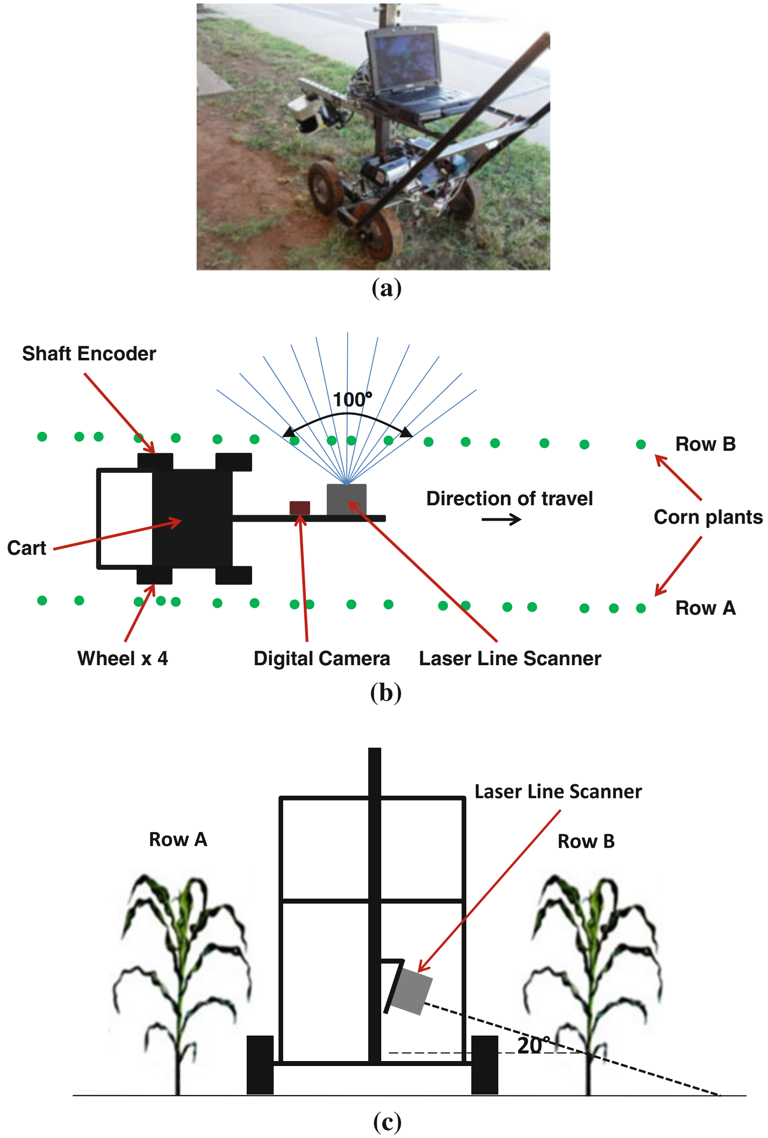

Fig. 1 Laser line-scan based corn plant location and spacing measuring system: (**a**) the cart with a laser line-scan sensor and other data acquisition devices. (**b**) Top view and (**c**) side view showing system operation

LabVIEW® (National Instruments Co., Austin, Texas, USA) was used to establish the communication between a laptop computer and the laser scanner, to receive data packages, to extract distance data and convert them from polar to Cartesian coordinates, and to save the data into a file with MS Excel format. The laser scanner scanned 100° and collected 401 distance measurements in 53.28 ms. With an average 0.447 m/s moving speed of the cart, the sensor moved about 2.4 cm within the time of a scan. This offset was ignored in this study. A 500 kbps baud rate was configured with a RS-422 connection and a serial to Ethernet convertor (DeviceMaster 500, Comtrol Co., New Brighton, Minnesota, USA) between the laser scanner and the laptop to ensure a sufficient data transfer rate.

A shaft encoder was mounted on one of the rear wheels and connected to a data acquisition card (USB 6008, National Instruments, TX) to obtain the location of each scan relative to a fixed start point. Hence, the data of each laser scan was location-stamped with a corresponding encoder reading. A video camera was mounted next to the laser line scanner to record a video of each trial which could be used later to verify the measurements of the laser line scanner.

Field experiment setup

The field experiment was conducted at Lake Carl Blackwell, near Stillwater, OK, in June and July of 2011. Data were collected from two 10-m long rows, each containing 50 corn plants, at the V8 and V10 growth stages. Three trials were conducted on each row at the V8 growth stage. Due to equipment malfunctions, only the data from two trials was used on row 1 at the V10 growth stage. Figure 2 shows the field setup for the data acquisition platform. The cart with the developed data acquisition platform was manually pushed between corn rows. The horizontal distance between the sensor and the corn row varied from 34 to 48 cm due to the deviation of the cart from the center line between rows. Since

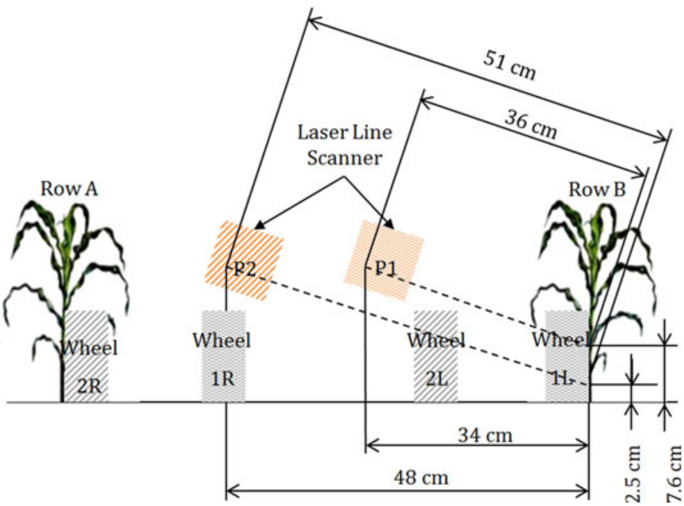

Fig. 2 Illustration of the cart's deviation between rows (not to scale): Case 1 (see *P1*) was when the cart was the closest to plant *row B* and Case 2 (see *P2*) was when the cart was the furthest to plant *row B*. Designations *1L* and *2L* indicated the positions of *left wheel*, and *1R* and *2R* indicated the positions of *right wheel* in these two cases, respectively

the laser scanner was mounted with a downward angle, when the cart travelled between the rows, the actual distance reading of the central point of a laser scan was between 36 and 51 cm. The sensor was mounted at a height so that, with this travel distance, the sensing plane on the plant stalks was between 2.5 and 7.6 cm above the plant roots. Manual location measurements were taken for the 100 plants and used as ground truth.

Data processing algorithms

Figure 3 shows a flowchart of the main data processing algorithm for locating corn stalks. Shaft encoder data of each scan were pre-processed so that it could be synchronized with ground truth measurement. For each scan, after eliminating the soil background, potential stalk clusters were classified and each was registered with corresponding stalk clusters from previous scans if they were identified as the same plant. Except for the most recent plant entering into the sensor's field of view during movement, each cluster in the current scan not corresponding to any of the clusters from previous scans were treated as noise. The final location of each recognized plant was calculated as the mean of the position measurements in all related scans. All data processing algorithms were developed in MATLAB® (MathWorks Inc., Natick, Massachusetts, USA).

Fig. 3 Flowchart of the main data processing algorithm for locating corn stalks

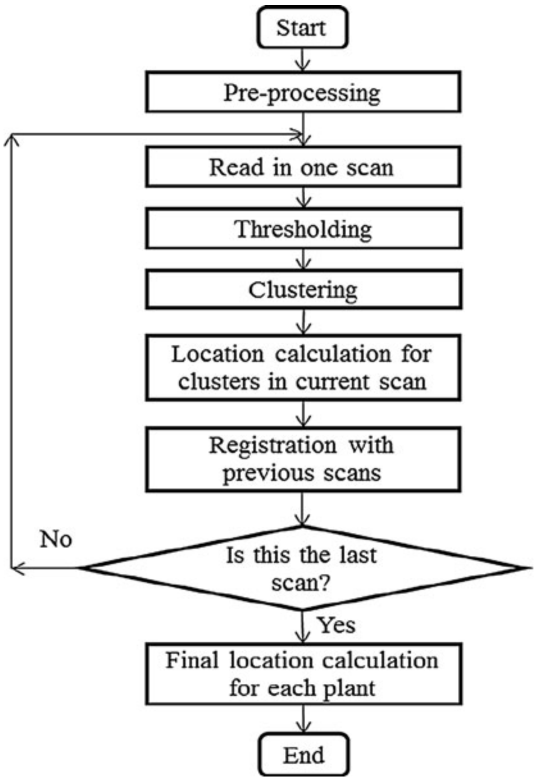

Synchronization of shaft encoder data and ground truth measurement

A pre-processing step was conducted on the shaft encoder data to synchronize it with ground truth measurements so that the system could be evaluated. Shaft encoder readings provided location of each laser scan. They were critical for in-row plant registration. The quality of the shaft encoder readings depended on the rotation of the wheel to which the encoder roller was attached. Intermittent rotation due to obstacles or uneven soil surface was unavoidable in a field experiment and could reduce positional accuracy. To partially correct for these deviations, encoder readings of each trial were stretched evenly along the entire row so that they would have an equal total length in between the 1st and 50th plants.

Thresholding

Figure 4a shows a typical scan after conversion to Cartesian coordinates. The sensor (gray square box) was at the origin of the local coordinates when this scan was taken. The clusters within 36–51 cm of the vertical axis of the coordinates corresponded to plant stalks. Other data points were the reflections from the soil background, leaves or other interfering objects and considered as noise. A thresholding process was conducted to eliminate noise data points that were not within the normal 36–51 cm range of the sensor as the cart travelled down the row.

Clustering

A clustering algorithm was implemented to identify potential stalk clusters based on the density variation of the line scan data. This algorithm was adapted from the density-based spatial clustering of applications with noise (DBSCAN) described by Ester et al. 1996.

Three parameters must be pre-defined in this algorithm: ε was the range in which a core point searched for a neighbor point to form a cluster and was set as a specific value no less than 0.85 cm according to the distance the core point was away from the origin; MinPts was the minimum number of data points needed to identify a cluster and was set as five; MaxPts was the maximum number of data points to be included in a cluster and was set as 25. These values were determined by trial and error in this study.

The value of radius ε in which a core point searched for its neighbors was not the same for every core point in the developed clustering algorithm. It varied based on the distance a data point was away from the origin. This was necessary because the radially collected data of the laser line scanner resulted in a higher density of data points near the scanner. The section area of a laser beam at a data point was calculated based on the divergence angle of the laser beam and the distance between that data point and the origin. The ratio of this section area to the section area of a laser beam at 44-cm away from the origin (cart centered between two rows) was obtained. It was used to multiply the minimum value of ε (which was 0.85 cm in this study) to be the specific ε value for that data point. The adjustable searching range ε made the clustering more accurate.

The values of MinPts and MaxPts were selected by assuming that the stalk diameters measured in this study would not be less than 1 cm or greater than 5 cm at both of the V8 and V10 growth stages. If the cart was moving along the center line between rows, a 5 cm or a 1 cm object would form a 25-point cluster or a five-point cluster at the central point of a laser scan when the sensing resolution was set as 0.25°. Hence, MinPts was set as five and MaxPts was set as 25.

Fig. 4 Illustration of clustering algorithm for stalk identification. (**a**) Typical line scan data after converting to Cartesian coordinates. *Circles* indicate reflectance data points; sensor was located at the origin (0, 0). (**b**) Clustering result of this scan: *1–5* were the identified clusters

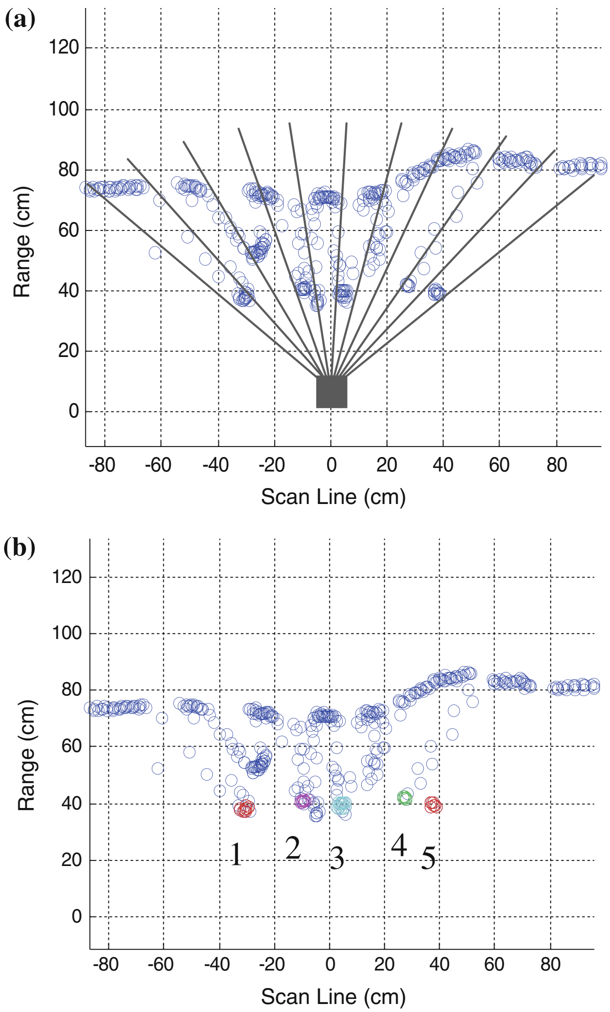

The clustering algorithm included the following steps:

1. All points in a dataset were initially marked as unvisited. The algorithm randomly started from one of the unvisited points p in the dataset and marked it as a visited point.
2. Made p a core point and searched for neighboring points within a radius ε. If no points were found within that range, marked p as noise and went back to step 1; otherwise, a new cluster was found consisting of p and its neighbors.
3. Each neighbor of the core point was assigned to the current cluster and was marked as visited. Each of point in the cluster was then treated as a core point and a search was conducted for its neighbors within a radius of ε. For each of the neighbor points found, step 3 was repeated until no new neighbors could be found.
4. Went back to step 1 until all points in the dataset had been visited.

5. Checked the size of each cluster. Only those clusters that had a size larger than MinPts and smaller than MaxPts were kept while others were treated as noise and eliminated.

The clustering algorithm developed in this study changed the criterion for identifying a point as a core point in a cluster expansion. In the referred algorithm (DBSCAN) a point was usually marked as a core point when it had more than three neighbors within a certain range; otherwise, the point was marked as noise. This made it possible to initially mark border points in a cluster as noise if the cluster had a narrow shape. Though DBSCAN changed them to cluster points later, this was inefficient if most of the points in a cluster were boarder points, which was the case when using a laser line scanner in plant stalk profiling. In the developed clustering algorithm, a cluster expansion started from a core point even if it had only one neighbor in a defined range.

Coordinate conversion

Two coordinate systems were involved in data processing—a local coordinate system and a ground coordinate system. Data from each scan had unique local coordinates due to the movement of the cart down the row. The origin of each local coordinate system was located at the laser source inside the laser line scanner. The *y-local* axis of each of the local coordinate system was along the midpoint of the sensor's field of view and increased with the distance away from the sensor; the *x-local* axis was perpendicular with *y-local* axis and increased to the right of the sensor. The origin of ground coordinates was at the start of each trial where the encoder reading was zero. The *x-ground* axis of the ground coordinates was parallel to the direction of sensor's travel; the *y-ground* axis was parallel to local coordinate axis indicating the depth measurement. The local coordinates of a plant in a scan were finally converted to the ground coordinates making use of the specific encoder reading of that scan.

Scan registration/matching between scans

Multiple scans obtained for the same stalk from various points of view gave a better chance to correctly recognize a plant. With the sensor's configured field of view while traveling at 0.447 m/s during data acquisition, a stalk generally appeared in approximately 40 continuous scans. Although it might be interfered with or blocked by leaves and other debris in some scans, a stalk still had a high possibility to be recognized in the rest of the scans. In order to match clusters from multiple scans corresponding to the same plant stalk, a scan registration procedure was implemented based on the difference of shaft encoder readings between scans.

Figure 5 is an illustration of this scan registration process. Assume scan # j was a current scan, scan # i was a previous scan, three clusters were shown in both scans, and the difference between encoder readings of these two scans was *d*. The developed algorithm used cluster locations in the current scan and *d* to calculate estimated cluster locations in the previous scan. It then searched for corresponding clusters within a small buffered search area around that estimated location for each cluster. The buffered search area was set as ±6 cm in this study by trial and error. If multiple corresponding clusters were found within that range for a cluster in the current scan, the one closest to the estimated location in the previous scan was selected. The first scan was exempted from registration. The clusters recognized in the first scan were assigned as plant stalks in incremental indices starting from one.

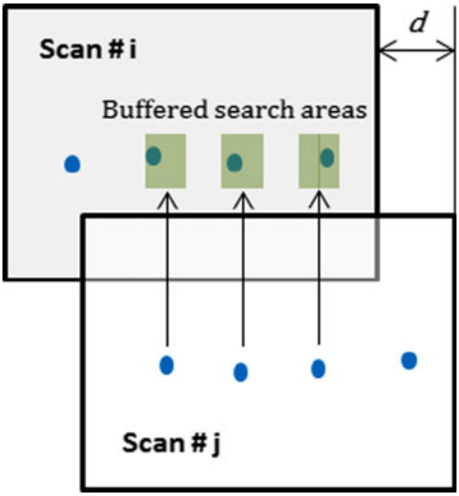

Fig. 5 Illustration of the scan registration algorithm

Registration started from the second scan and each scan could only register with the previous scans in order to meet the requirement by a real-time processing system. For each cluster in the current scan, the algorithm searched backward through up to thirty previous scans to find a matching cluster. Once a matching cluster was found, the one in the current scan was assigned to the same cluster index as the cluster in the previous scan; otherwise, the cluster in the current scan was marked as not being matched. Finally, all the unmatched clusters were checked to see if there was a cluster which newly entered into the sensor's field of view. If there was one, a new cluster index was assigned to it. At the end of the process, all the unmatched clusters were marked as noise clusters.

The final location of a recognized plant stalk was the mean location of all clusters with the same index in different scans. Estimated locations which were within 5 cm of each other had a high likelihood of corresponding to a stalk and a sheath (Fig. 6). Sheath interference was compensated for by averaging the locations of two estimated locations less than 5-cm apart into one location.

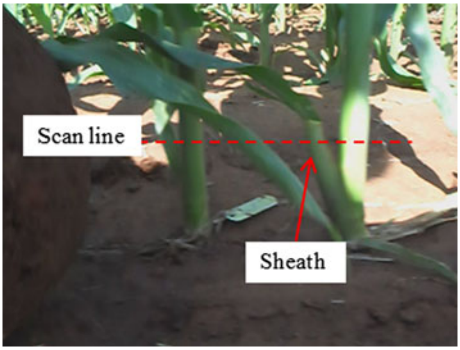

Fig. 6 Sheath interference with stalk locations

System performance evaluation

System performance was evaluated by comparing its measurements to ground truth data which was measured manually by a ruler for each plant row. Errors in plant counting, plant location estimate and interplant spacing estimate were analyzed.

Plant counting

Three errors were defined for evaluating system's performance on plant counting: the false negative counting error (FNEr) (Eq. 1), false positive counting error (FPEr) (Eq. 2), and total counting error (TEr) (Eq. 3):

$$\text{FNEr} = \frac{\text{Missing count}}{\text{Ground truth count}} \times 100\,\% \tag{1}$$

$$\text{FNEr} = \frac{\text{Adding count}}{\text{Ground truth count}} \times 100\,\% \tag{2}$$

$$\text{TEr} = \text{FNEr} - \text{FPEr} \tag{3}$$

If no plant was identified within ± 10 cm from the ground truth location of an actual plant, there was a false negative count for that actual plant. Similarly, if no actual plant was located within ± 10 cm of the location of an identified plant, this resulted in a false positive count. Only the recognized plant closest to (and within ± 10 cm) the location of an actual plant was a valid count; multiple counts of an actual plant were treated as false positive counts. The total counting error was equal to the sum of the false negative error and false positive error. These errors were calculated for each of the two rows at each growth stage. The SAS (SAS Institute, Cary, North Carolina, USA) General Linear Model procedure (GLM) was used to test for significant differences in FNEr, FPEr and TEr between the V8 and V10 growth stages.

Plant location estimation

The RMSE was calculated between the manually measured ground truth locations and those measured by the developed system for all correctly recognized plants in each row at each growth stage. In this analysis, locations corresponding to false negative counts were eliminated from ground truth locations in each trial while locations corresponding to false positive counts were eliminated from system measured locations. The significant difference in plant location estimates between the V8 and V10 growth stages was also tested using GLM procedure in SAS.

Plant spacing estimation

Another parameter to investigate plant location error was the error of interplant spacing estimates. Interplant spacing was calculated as the difference between every recognized plant pair in a row excluding false positive and false negative counts for each trial. The spacing of the two plants at each side of a false negative count was eliminated from the system measured spacing in order to correlate with the manually measured spacing. The RMSE of estimated spacing of all identified plants was calculated for each row in each trial and compared to manually measured spacing. If two successive plants were only correctly recognized in one trial, their spacing was compared to ground truth data; if two successive plants were correctly recognized in different trials, the corresponding spacing measurements were averaged before comparing to ground truth data.

Results and discussion

Plant counting error

At the V8 growth stage, an averaged 2.0 % (SD = 1.6 %) FNEr, an averaged 22.0 % FPEr and an averaged 24.0 % (SD = 6.9 %) TEr were achieved. At the V10 growth stage, a 3.0 % (SD = 1.0 %) FNEr, a 7.0 % (SD = 3.0 %) FPEr, and a 10.0 % (SD = 4.0 %) TEr were achieved (Table 1).

No significant difference was found in FNEr ($F_{1,6} = 0.50$, $p = 0.51$) and TEr ($F_{1,6} = 5.51$, $p = 0.057$) between the V8 and V10 growth stages. While a significant difference was found in FPEr between V8 and V10 growth stages ($F_{1,6} = 7.61$, $p = 0.033$). At V8 growth stage, false positive errors were larger than false negative errors for both rows; while at the V10 growth stage, false positive errors decreased and false negative errors increased. The large false positive error at V8 growth stage was primarily due to weed interference which prevented the system from differentiating weeds from stalks (Fig. 7a). Row 2 had larger errors than row 1 at V8 growth stage. The recorded video indicated more weed interference for row 2 than row 1 at that time. This suggested that the system developed in this study should be used in a weed controlled plot. A higher sensing height to avoid the weed area might help although interference from leaves on the stalk could offset improvements. At the V10 growth stage, weeds had been treated with herbicide so false positive errors decreased; however, most of the lower leaves were dehydrated and laid over the stalk (Fig. 8). A leaf cluster often had a larger size (>25 data points) than a stalk cluster. This was used by the algorithm to differentiate the leaf clusters from the stalk clusters. Attached leaves prevented the sensor from seeing the actual shape of the stalks resulting in more false negative errors. At the V8 growth stage, most of the lower leaves were still vital and standing up.

The number of plants identified in each trial was used to assess the repeatability of system estimates. At the V8 growth stage, 49 out of 50 plants (98.0 %) were identified in all trials in row 1 though all 50 plants were identified in at least one trial; 46 plants out of 49 plants (93.9 %) were identified in all trials in row 2 excluding a plant located 3 cm apart from one of its neighbors though the other 48 plants were identified in at least one trial. At the V10 growth stage, 47 out of 50 plants (94.0 %) were identified in valid trials in row 1 though all 50 plants were identified in at least one trial.

Table 1 Errors of plant counting and stalk location estimates compared to ground truth data

	FNEr (%)	FPEr (%)	TEr (%)	RMSE of location estimate (cm)	RMSE of spacing estimate (cm)
Row 1, V8	1.3 (0.94)*	16.0 (1.6)	17.3 (0.94)	1.9 (0.2)	2.1 (0.3)
Row 2, V8	2.7 (1.9)	28.0 (2.8)	30.7 (2.5)	2.8 (0.3)	2.9 (0.8)
Row 1, V10	3.0 (1.0)	7.0 (3.0)	10.0 (4.0)	2.6 (0.2)	2.0 (0.1)

* Numbers in the parenthesis represent standard deviation

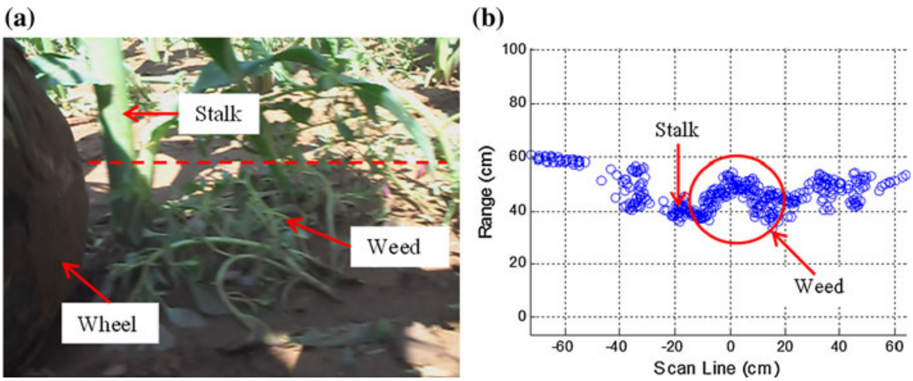

Fig. 7 Weed interference at the V8 growth stage. (**a**) A stalk with weed interference in row 2. (**b**) Corresponding laser line scan data

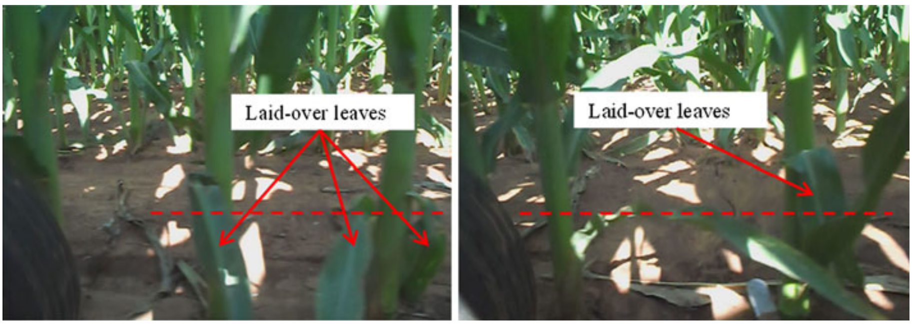

Fig. 8 Typical laid-over leaf interference at the V10 growth stage

Plant location and spacing error

The RMSEs of system measured plant locations were 2.3 cm (SD = 0.5 cm) and 2.6 cm (SD = 0.2 cm) for the V8 and V10 growth stages, respectively, for those correctly identified stalks in each row at each growth stage. No significant difference was found in RMSE of location estimate between the V8 and V10 growth stages ($F_{1,6} = 0.29$, $p = 0.61$) which demonstrated the repeatability in location estimate at two different growth stages of the system. This plant location estimate error was relatively small compared with the 20.2 cm (SD = 10.6 cm) interplant spacing which is discussed in the next section.

Factors contributing to errors in plant location estimates included errors from data acquisition, data processing and sheath and leaf interference. Small diameter wheels on the cart likely caused some inaccuracy at some locations due to the uneven terrain in the field. The correction for encoder readings in data pre-processing distributed the encoder error evenly to every scan in a trial. This problem would be reduced if the encoder was mounted on a wheel with a larger contact area with the soil surface. Subjective error was induced in the manual measurement of plant locations. In addition, corn plants were not perfectly vertical during growth stages which caused inconsistency between manual and system measurements.

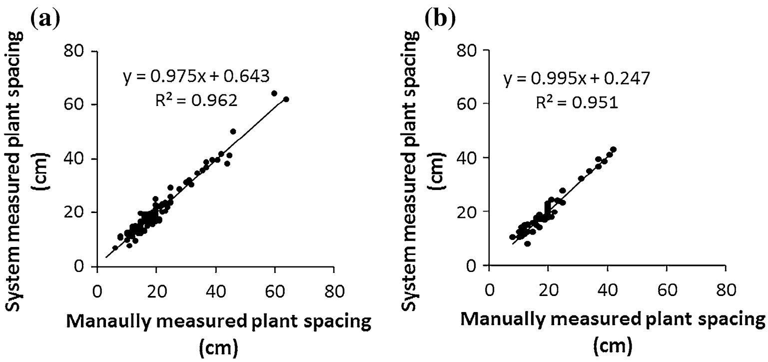

Fig. 9 Comparison between system measured interplant spacing and manually measured interplant spacing (**a**) at the V8 growth stage (n = 96) and (**b**) at the V10 growth stage

Interplant spacing estimated by the system was highly correlated to ground truth data. Comparison between them at the V8 growth stage resulted in RMSE of 2.5 cm (SD = 0.8 cm), an R^2 of 0.962 and a slope of 0.975 with an intercept of 0.643 in the regression equation (Fig. 9a). At the V10 growth stage, this comparison resulted in RMSE of 2.0 cm (SD = 0.1 cm), an R^2 of 0.951 and a slope of 0.995 with an intercept of 0.247 (Fig. 9b). The slopes were close to one and the intercepts were close to zero in both regression equations.

Distribution of manually and system measured interplant spacing was also investigated. Manually measured interplant spacing had a mean of 20.2 cm (SD = 10.6 cm); while those measured by the developed system had a mean of 20.6 cm (SD = 11.0 cm) at the V8 growth stage (Fig. 10a). Manually measured interplant spacing had a mean of 19.6 cm (SD = 8.5 cm); while those measured by the developed system had a mean of 19.8 cm (SD = 8.6 cm) at the V10 growth stage (Fig. 10c). The similarity in the means and standard deviations of the system measurements with the ground truth data demonstrated the repeatability of the system developed in this study.

The errors of the system measured interplant spacing had means of 0.1 cm (SD = 1.9 cm) and 0.1 cm (SD = 1.9 cm) at the V8 and V10 growth stages, respectively (Fig. 10b, d). Shapiro–Wilk normality tests were conducted to test the normality of the error distributions at the two growth stages. There was no significant evidence to reject the null hypothesis that they were normally distributed (SWstatistic = 0.97, $p = 0.82$ for V8; SWstatistic = 0.99, $p = 0.34$ for V10; $\alpha = 0.05$) which demonstrated the reliability of the system measurements. However, the slightly positive skewed shape in the error distribution plot of the V10 stage (Fig. 10d) indicated that there was an error source. It was very likely associated with the pre-processing procedure in data processing in which the encoder reading was stretched in order to be synchronized with the ground truth data. The stretch ratio was larger in the V10 than that in the V8 growth stage because the drought soil condition in the V10 growth stage caused more missing encoder counts. This suggested an improvement on the data acquisition platform with a better wheel encoder mechanism in the future.

Evaluation of overall system performance

The RMSEs of interplant spacing measurements were 2.5 cm (SD = 0.8 cm) at the V8 growth stage and 2.0 cm (SD = 0.1 cm) at the V10 growth stage. These results were at a

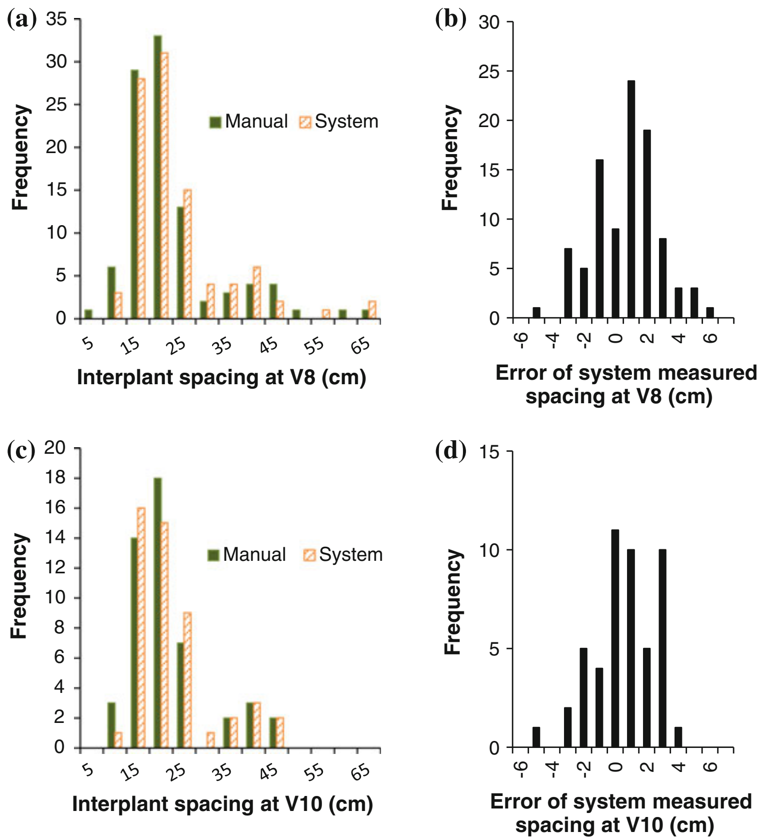

Fig. 10 Histograms of (**a**) manually and system measured interplant spacing, and (**b**) error distribution of system measured interplant spaces at the V8 growth stage; (**c**) manually and system measured interplant spacing and (**d**) error distribution of system measured interplant spaces at the V10 growth stage

centimeter or a tenth of a centimeter level, which were smaller or close to the agronomic spacing findings at a centimeter level described by Krall et al. (1977) and Lauer and Rankin (2004). This indicated that the developed system could be used to provide useful plant location and spacing information from an agronomic point of view.

In summary, the developed approach had its unique features comparing with others from previous research. Firstly, it was suitable for sensing corn plant location and spacing at mid-growth stage. Previous work based on 2D imaging and collected data from the top of the canopy could only be applied at early corn growth stages. At the mid-growth stage, the corn canopy might overlap with each other, thus made it difficult to differentiate individual plant. Secondly, the developed approach could reduce interference from leaves and other objects by scanning a plant multiple times. This greatly increased the possibility to identify each plant and improved the accuracy on corn location and spacing measurements when compared with 1D ranger sensors. Thirdly, the developed, laser-scanner-based approach acquired less data for plant measurements; hence, led to faster processing and communication speed and low demands on data processing and storage comparing with 2D imaging methods. This was very important for real-time, field implementation.

Conclusions

A system based on laser line-scan technique was developed and tested to estimate corn plant locations and interplant spacing at mid growth stages. The field experiment results demonstrated that:

- Using a laser line scanner to identify corn plant stalks from different points of view on-the-go is a feasible method for plant counting, location and spacing measurement. The current system achieved 24.0 and 10.0 % of mean total errors in plant counting at the V8 and V10 growth stages, respectively. The mean RMSEs of the system measured locations for correctly identified plants were 2.3 and 2.6 cm at the V8 and V10 growth stages, respectively. Comparison between system measured and manually measured interplant spacing had R^2 of 0.962 and 0.951 for the V8 and V10 growth stages, respectively.
- The system can be enhanced for better performance in the future. Redesign of the wheel encoder mechanism will increase the reliability in data acquisition. Data processing algorithm can also be modified on reducing errors from interfering factors and fine-tuning parameter values.
- For practical deployment, the developed system can be upgraded by using a laser scanner with a faster data communication rate and an on-board fast microprocessor-based data-logging system to accommodate the travel speed of a tractor (e.g. 6–10 kmph).

Acknowledgments The authors would like to thank Jeremiah Mullock and Natasha Macnack in Department of Plant and Soil Sciences for their help in plot preparation and manual measurement. Appreciation also goes to Wesley Porter, Jorge Rascon, Marshall Oldham, Bin Li, Aaron Franzen and Yongbo Wan in Department of Biosystem and Agricultural Engineering for their help in field test which made this project successful.

References

Birrell, S. J., & Sudduth, K. A. (1995). *Corn population sensor for precision farming*. ASAE paper No. 951334. St. Joseph, Michigan.

Dworak, V., Selbeck, J., & Ehlert, D. (2011). Ranging sensor for vehicle-based measurement of crop stand and orchard parameters: a review. *Transactions of the ASABE, 54*(4), 1497–1510.

Ester, M., Kriegel, H., Sander, J., & Xu, X. (1996). *A density-based algorithm for discovering clusters in large spatial databases with noise. Proceedings of 2nd International Conference on Knowledge Discovery and Data Mining* (pp. 226–231). Menlo Park, CA: AAAI Press.

Gauer, L. E., Grant, C. A., Gehl, D. T., & Bailey, L. D. (1992). Effects of nitrogen fertilization on grain protein content, nitrogen uptake, and nitrogen use efficiency of six spring wheat (*Triticum aestivum* L.) cultivars, in relation to estimated moisture supply. *Canadian Journal of Plant Science, 72*, 235–241.

Heege, H., Reusch, S., & Thiessen, E. (2004). *Systems for site-specific on-the-go control of nitrogen top-dressing during spreading. Proceedings of the 7th International Conference on Precision Agriculture and Other Precision Resources Management* (pp. 133–147). Minneapolis, MN.

Huang, Y., Lan, Y., Ge, Y., Hoffmann, W. C., & Thomson, S. J. (2010). Spatial modeling and variability analysis for modeling and prediction of soil and crop canopy coverage using multispectral imagery from an airborne remote sensing system. *Transactions of the ASABE, 53*(4), 1321–1329.

Hummel, J. W., Drummond, S. T., Sudduth, K. A., & Krumpelman, M. J. (2002). *Sensing systems for site-specific assessment of corn plants. Proceedings of the 6th International Conference on Precision Agriculture (unpaginated)*. Madison, WI: ASA, CSSA, and SSSA.

Krall, J. M., Esechie, H. A., Raney, R. J., Clark, S., TenEyck, G., Lundquist, M., et al. (1977). Influence of within-row variability in plant spacing on corn grain yield. *Agronomy Journal, 69*, 797–799.

Lauer, J. G., & Rankin, M. (2004). Corn response to within row plant spacing variation. *Agronomy Journal, 96*, 1464–1468.

Li, H., Worley, S. K., & Wilkerson, J. B. (2009). Design and optimization of a biomass proximity sensor. *Transactions of the ASABE, 52*(5), 1441–1452.

Luck, J. D., Pitla, S. K., & Shearer, S. A. (2008). *Sensor ranging technique for determining corn plant population.* ASABE paper No. 084573. St. Joseph, Michigan.

Martin, K. L., Hodgen, P. J., Freeman, K. W., Melchiori, R., Arnall, D. B., Teal, R. K., et al. (2005). Plant-to-plant variability in corn production. *Agronomy Journal, 97*, 1603–1611.

Martin, K., Raun, W., & Solie, J. (2012). By-plant prediction of corn grain yield using optical sensor readings and measured plant height. *Journal of Plant Nutrition, 35*, 1429–1439.

Nichols, S. W. (2000). *Method & apparatus for counting crops*. U.S. Patent No. 6073427.

Raun, W. R., & Johnson, G. V. (1995). Soil–plant buffering of inorganic nitrogen in continuous winter wheat. *Agronomy Journal, 87*, 827–834.

Raun, W. R., & Johnson, G. V. (1999). Improving nitrogen use efficiency for cereal production. *Agronomy Journal, 91*, 357–363.

Saeys, W., Lenaerts, B., Craessaerts, G., & De Baerdemaeker, J. (2009). Estimation of the crop density of small grains using LiDAR sensor. *Biosystems Engineering, 102*(1), 22–30.

Shrestha, D. S., & Steward, B. L. (2003). Automatic corn plant population measurement using machine vision. *Transactions of the ASABE, 46*(2), 559–565.

Shrestha, D. S., & Steward, B. L. (2005). Shape and size analysis of corn plant canopies for plant population and spacing sensing. *Transactions of the ASABE, 21*(2), 295–303.

Sowers, K. E., Pan, W. L., Miller, B. C., & Smith, J. L. (1994). Nitrogen use efficiency of split nitrogen applications in soft white winter wheat. *Agronomy Journal, 86*, 942–948.

Tang, L., & Tian, L. F. (2008a). Real-time crop row image reconstruction for automatic emerged corn plant spacing measurement. *Transactions of the ASABE, 51*(3), 1079–1087.

Tang, L., & Tian, L. F. (2008b). Plant identification in mosaicked crop row images for automatic emerged corn plant spacing measurement. *Transactions of the ASABE, 51*(6), 2181–2191.

Thorp, K. R., Steward, B. L., Kaleita, A. L., & Batchelor, W. D. (2008). Using aerial hyperspectral remote sensing imagery to estimate corn plant stand density. *Transactions of the ASABE, 51*(1), 311–320.

Wangler, R. J., Fowler, K. L. & McConnell, R. E. (1994). *Object sensor and method for use in controlling an agricultural sprayer*. U. S. Patent No. 5278423.

Wei, J., & Salyani, M. (2004). Development of a laser scanner for measuring tree canopy characteristics. Phase 1. Prototype development. *Transactions of the ASABE, 47*(6), 2101–2107.

Wei, J., & Salyani, M. (2005). Development of a laser scanner for measuring tree canopy characteristics. Phase 2. Foliage density measurement. *Transactions of the ASABE, 48*(4), 1595–1601.